Environ Geochem Health
https://doi.org/10.1007/s10653-022-01465-9

ORIGINAL PAPER

Preindustrial levels and temporal enrichment trends of mercury in sediment cores from the Gulf of Thailand

Tanakorn Ubonyaem · Sujaree Bureekul · Chawalit Charoenpong · Pontipa Luadnakrob · Penjai Sompongchaiyakul

Received: 28 September 2022 / Accepted: 19 December 2022

Abstract Four sediment cores in the middle of Gulf of Thailand (GOT) and one core close to Bang Pakong River mouth were examined for total mercury (T-Hg) using direct thermal decomposition coupled with the atomic absorption spectrometry (DTD-AAS) method and acid digestion (acid-CVAAS) method, and sediment chronologies using ^{210}Pb dating. T-Hg in the river mouth core ranged 44.49–52.76 µg/kg and higher than the cores from the middle of GOT (18.26–36.68 µg/kg). The age span obtained from the cores dated back to the 1940s with the sediment accumulation rates of 0.15–0.76 cm/year. The preindustrial levels of T-Hg showed an initial slow increase followed by a rapid elevation since the 1960s which marked the start of the industrialized period in the country. To this end, we posit that T-Hg in the GOT sediment can be attributed to not only land-based sources but also offshore activities including petroleum exploration and frequent accidental oil spills.

Keywords Total mercury · Gulf of Thailand · ^{210}Pb dating · CVAAS · DTD-AAS · Petroleum exploration

Introduction

Mercury (Hg) is a highly toxic metal especially as a potent neurogenic toxin. In seawater, Hg can be rapidly scavenged by particles. Subsequently, it descends along with sinking particles and accumulates in the sediment. However, Hg is redistributed back to the overlying water and becomes bioavailable according to geochemical conditions of the sediments (Braune et al., 2015; Fitzgerald et al., 2007; Gworek et al., 2016; Zhu et al., 2018). Organic Hg (Org-Hg), e.g., monomethylmercury and dimethylmercury, are the most toxic species of Hg (Gworek et al., 2016; Issaro et al., 2009; Shoham-Frider et al., 2012). However, Org-Hg typically made up less than 1% of the total mercury (T-Hg) in sediment (Agah et al., 2009; Gilmour et al., 2018; Issaro et al., 2009; Shoham-Frider et al., 2012; Wang et al., 2009; Zhao et al., 2019). Only in rare occasions that Org-Hg constitutes a large portion of Hg found in sediment. Gilmour et al. (2018) investigated Hg released from a mercury-cell

Supplementary Information The online version contains supplementary material available at https://doi.org/10.1007/s10653-022-01465-9.

T. Ubonyaem · S. Bureekul · C. Charoenpong · P. Sompongchaiyakul (✉)
Department of Marine Science, Faculty of Science, Chulalongkorn University, Bangkok 10330, Thailand
e-mail: penjai.s@chula.ac.th

P. Luadnakrob
Southeast Asian Fisheries Development Center, Training Department, Samut Prakan 10290, Thailand

P. Sompongchaiyakul
Research Program on Remediation Technologies for Petroleum Contamination, Center of Excellence on Hazardous Substance Management (HSM), Chulalongkorn University, Bangkok, Thailand

Published online: 30 January 2023

chlor-alkali plant in the tidal wetland and saltmarsh soils and found that Org-Hg was up to 10% of T-Hg in sediment. Since Org-Hg hardly makes up a sizeable fraction of sedimentary Hg inventory in normal sediment and the tedious analytical processes required for the analysis of extremely high toxic methylmercury, the T-Hg analysis is an appropriate option to be used as a rapid indicator for Org-Hg estimation in routine monitoring.

Conventional analysis of T-Hg in sediment involves sample preparation via digestion by hot acid as reviewed by Issaro et al. (2009) includes the use of nitric acid (HNO_3), sulfuric acid (H_2SO_4), hydrochloric acid (HCl), perchloric acid ($HClO_4$), hydrofluoric acid (HF), and aqua regia mixture. Once Hg extraction into aqueous solutions is complete, several options are available for Hg determination. Cold vapor atomic adsorption spectrometry (CVAAS) and cold vapor atomic fluorescence spectrometry (CVAFS) with or without gold amalgamation are the most frequently chosen for detecting trace amount of Hg since both techniques provide excellent sensitivity (US Elezz et al., 2018; EPA, 1994, 2002; Franklin et al., 2012; Huber & Leopold, 2016; Kan et al., 2006; Leng et al., 2013).

To date, direct thermal decomposition coupled with atomic absorption spectrometry (DTD-AAS) has become more preferable approach since no digestion is required (Issaro et al., 2009). This DTD-AAS technique was first introduced two decades ago (US EPA, 1998). The technique showed excellent results with the various certified solid reference materials (US EPA, 1998; Homira et al., 2009). The DTD-AAS approach has been recommended for T-Hg analysis in biological samples in many previous works (Cizdziel et al., 2002; Panichev & Panicheva, 2015).

The Gulf of Thailand (GOT), a semi-enclosed bay encompassed by the land of Thailand, Cambodia, Vietnam, and Malaysia (Fig. 1), receives freshwater discharge including anthropogenic pollutants from surrounded land-based sources to the north. Moreover, a large number of petroleum exploration/production activities are located in the middle of the GOT (DMF, 2018) since late 1960s, a few years after the beginning of the industrialized period in Thailand. Unfortunately, the petroleum source in the GOT bears high T-Hg content (Charoensawadpong et al., 2018; Pongsiri, 1997) and is likely to act as a marine-based source of T-Hg accumulated in the GOT sediment

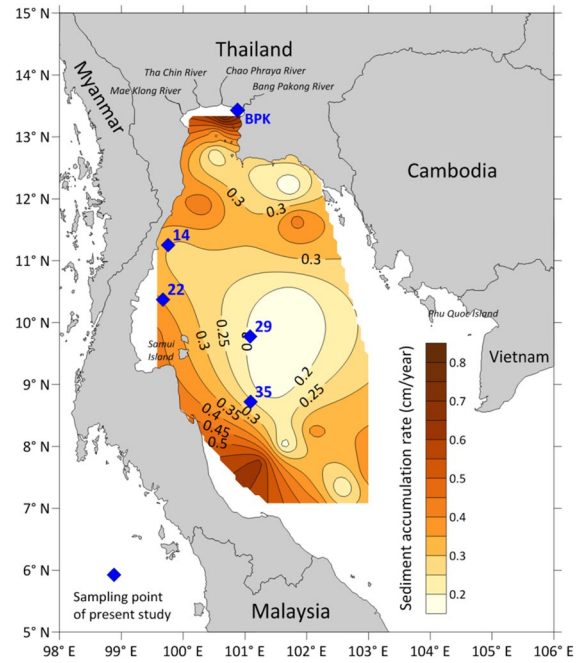

Fig. 1 The locations of sediment cores collected in this study are indicated by the blue diamonds. A contour map shows a reproduction of sediment accumulation rates (SAR) based on data from Srisuksawad et al. (1997)

(Buakaew, 2007; Liu et al., 2016; Sansittisakunlird, 2014; SEAFDEC, 2013). Therefore, the temporal change of T-Hg in sediment core samples is necessary to explain the contamination history of T-Hg in the GOT sediment. One previous work on the historical elevation of T-Hg in the upper layer of the GOT sediment core collected in the middle of GOT was carried out by Liu et al. (2016). However, their results did not reflect any observable trend accompanying T-Hg accumulation from both land-based and marine-based sources exploited after the industrial development. This could partly be explained by the sub-sectioning of every 10 cm sediment layer which was too widely spaced leading to the insufficient resolution in sediment chronology since sedimentation rates in the middle of GOT were estimated to be about 0.2 cm/year (Srisuksawad et al., 1997).

To close such gaps in our understanding, this current investigation used five sediment cores from GOT to determine the historical change in T-Hg concentration. Four sediment cores were retrieved from different location in the GOT representing marine-based sources, and one sediment core

collected close to Bang Pakong River mouth in the upper GOT, representing land-based sources. The T-Hg in sediment was analyzed using DTD-AAS method and sediment ages were determined by ^{210}Pb dating. Since all earlier studies on T-Hg content in the GOT sediment has been investigated by a conventional method or acid digestion (Buakaew, 2007; Liu et al., 2016; Sansittisakunlird, 2014; SEAFDEC, 2013; Thongra-ar et al., 2008). To ensure that our results can be compared with the previous works, we conducted an additional comparison between DTD-CVAAS and the classical acid digestion-CVAAS on selected sediment samples. Other sedimentology and geochemical characterization (i.e., grain size, carbonate and organic carbon contents) were also conducted; these parameters have been identified as the major controlling factors of metal distribution (Chakraborty et al., 2015; Dou et al., 2013; Gonzalez-Raymat et al., 2017; Kelly & Rudd, 2018).

Materials and methods

Sample collection

Four sediment cores (Fig. 1, Supplementary Table S1) were collected during 16 August to 11 October 2018 under the "Collaborative Research Survey on Marine Fisheries Resources and Marine Environment in the Gulf of Thailand" aboard M.V. SEAFDEC-2. Each core sample was retrieved from a box corer (30 cm × 30 cm × 60 cm) with an acrylic pipe (65 cm × 10 cm i.d.). The sub-section of sediment core was performed on board at 1-cm intervals. For these four cores, Hg analysis was done only at 2–4 cm intervals. On the other hand, the Bang Pakong sediment core was collected in 2020 using a gravity corer on the R.V. Kasetsart-1 and was sub-sectioned at 2-cm intervals, and every other section was analyzed for T-Hg. All subsamples were immediately frozen at − 20 °C. Back in the laboratory, all sediments were freeze-dried. After that, they were sieved through 2 mm mesh to remove shells and larger particles. One portion of dry sediment was grounded and used for geochemical and T-Hg analyzes, while the intact portion was used for grain size composition analysis.

Sedimentology and geochemical analysis

The grain size of sediment sample was determined by wet sieving and sedimentation method following protocol outlined in (Sompongchaiyakul, 1989). Briefly, organic matter and carbonate content in the dry sediment were removed by using 25% H_2O_2 and 6 M HCl, respectively. Consequently, the sediment was wet sieving to separate sand (> 63 µm) and fine (< 63 µm) fraction. Calcium carbonate ($CaCO_3$) in the sediment samples were determined based on acid dissolution. The remained unused acid was titrated by basic solution (Sompongchaiyakul, 1989). Readily oxidizable organic carbon (ROOC) in sediment was determined based on modified Walkley–Black Method (Loring & Rantala, 1992).

T-Hg analysis

Chemicals

All chemicals were of analytical reagent grade. High purity HCl and HNO_3 were prepared by sub-boiling distillation using Berghof distillacid BSB-939-IR. Deionized water (> 17.8 MΩ·cm) was used to prepare aqueous reagents and standard solutions.

Analysis of T-Hg by DTD-AAS

Analysis of T-Hg by DTD-AAS was performed using MA-3000 mercury analyzer (Nippon Instruments Corporation, NIC) which is in compliance with US EPA method 7473 (US EPA, 1998). Approximately 100 mg of dry sediment was loaded into the machine and decomposed according to programmable high temperature under oxygen gas (> 99% purity). Standard solutions were prepared from 1014 mg/L $HgCl_2$ standard solution (Kanto Chemical, Japan), and the standard solution series was diluted with 0.01% (w/v) L-cysteine (98%, Nacalai tesque, Japan) in 0.2% (v/v) HNO_3 (Ultrapure, Kanto Chemical, Japan).

Analysis of T-Hg by acid-CVAAS

The acid-CVAAS method was modified from US EPA (2001) Appendix to Method 1631 using The PerkinElmer Flow Injection Mercury System (FIMS-400). Briefly, dry sediment was digested with cold aqua regia (HNO_3:HCl = 1:4 v/v) overnight (> 12 h), then

heated at 95 °C for 15 min by a heating block. The digested solution was made up to 40 mL with deionized water. Ten milliliters aliquot was added with 100 µL of 0.2 N BrCl. Prior to determination, 100 µL of 12% (w/v) $NH_2OH{\cdot}HCl$ was added to neutralize any excess BrCl. Standard solutions were prepared in the 0.1–10 µg/L range from $Hg(NO_3)_2$ 1000 ± 2 mg/L (Merck) and diluted with deionized water.

Quality assurance and quality control (QA/QC)

The analytical performance of the both Hg analyzers was investigated in terms of linear ranges and detection limits (Table S2). The limit of detection (LOD = 3SD) and limit of quantitation (LOQ = 10SD) values were calculated based on standard deviation (SD) of the ten repeated determination of the blank for DTD-AAS and for the lowest concentration of the standard (0.01 µg/L) for acid-CVAAS. Data variation is shown as percentage of relative percent difference value (%RPD) for DTD-AAS results (Table S4) and percentage of relative standard deviation (%RSD) for acid-CVAAS results (Table S5), respectively. The method validation was performed by analysis of two certified reference materials (CRMs), MESS-3 and PACS-2. Average recovery of the CRMs analysis was in the range of 95–100% (Table S3). Both methods provided excellent recovery and reproducible data (%RSD < 10), indicating the two methods have given reliable results in both accuracy and precision.

Sediment dating

Sample preparation and extraction

Total ^{210}Pb was indirectly determined through ^{210}Po, a grand-daughter isotope, using alpha spectrometry. Sediment samples were processed using an in-house method of the Department of Nuclear Engineering, Faculty of Engineering, Chulalongkorn University similar to that described in Begy et al. (2015). Briefly, 2 g of sediment powder spiked with calibrated ^{209}Po tracer prior to reflux in 20 mL conc. HNO_3 at 150 °C for 5 h, then evaporate to near dryness. After organic matter decomposition with 30% H_2O_2 at room temperature was done, 10 mL of conc. HNO_3 was added and refluxed repeatedly. The supernatant was diluted with 40 mL deionized water and adjusted pH to 7–8 with conc. ammonium hydroxide solution to allowing the co-precipiation of Po and iron oxide. The red iron oxide precipitate was re-dissolved in 6 M HCl and made volume to 50 mL with deionized water. 5 mL of 20% hydroxylamine, 2 mL of 5% sodium citrate, and 0.1 g of ascorbic acid were added and adjusted the pH of solution to 3. Subsequently, silver disk (diameter 7/8 inch) was submerged into the solution to allow the spontaneously deposition of Po on the disk at 90 °C for 3 h.

Model age derived from ^{210}Pb analyzes

Activities of ^{210}Po and ^{209}Po tracer on silver disk were measured in an alpha spectrometer (Octête Plus, ORTEC). Since ^{210}Po exists in secular equilibrium with ^{210}Pb, it is a suitable alternative nuclides for ^{210}Pb determination (Begy et al., 2015; Zaborska et al., 2007). Due to the lack of water content and sediment porosity information, the calculation of ^{210}Pb activities was based on the constant flux and constant sedimentation (CFCS) model (Bruel & Sabatier, 2020) as shown in the following equation:

$$^{210}Pb_{ex} = {}^{210}Pb_{ex(0)} \cdot e^{-\lambda t} \quad \text{with} \quad t = z/\mathrm{SAR}$$

where t is the age at z cm sediment layer below the surface, $^{210}Pb_{ex}$ is an unsupported or excess ^{210}Pb activity at depth z cm, $^{210}Pb_{ex(0)}$ is the $^{210}Pb_{ex}$ activity at the surface layer, and λ is ^{210}Pb decay constant. Subsequently, sediment accumulation rate (SAR; cm/year) was obtained from the following equation:

$$\mathrm{SAR} = -\lambda/a$$

where a is a slope from a linear regression of the logarithm of $^{210}Pb_{ex}$ vs. the depth profiles.

The $^{210}Pb_{ex}$ activities of each sediment layer in this work were estimated through the difference between total ^{210}Pb and supported ^{210}Pb activities, where the supported ^{210}Pb activities were estimated from average total ^{210}Pb activities at the bottom of each sediment core profile (Yeager et al., 2018).

Results and discussion

T-Hg in sediment; the DTD-AAS and acid-CVAAS methods comparisons

The results of T-Hg in 53 sediment samples (taken from 4 sediment cores in the GOT excluding core BPK) determined by DTD-AAS and acid-CVAAS were compared (Fig. 2 and in Supplementary data, Fig. S1). The ranges of T-Hg concentration obtained from DTD-AAS and acid-CVAAS methods were 16.19 to 32.95 and 15.97 to 34.17 µg/kg, respectively (Table S4 and S5 in Supplementary data). The acceptable precision was reported for both DTD-AAS (%RPD < 10) and acid-CVAAS (%RSD < 15). DTD-AAS provides a better detection limit and a wider range of analytical concentration (Table S2). LOD and LOQ reported for the DTD-AAS method were 0.01 and 0.05 µg/kg, respectively. While, the LOD and LOQ for the comparative acid-CVAAS method were reported at 0.80 and 2.72 µg/kg, respectively.

Pearson's correlation coefficient ($r = 0.9401$, p value < 0.001) and paired t-test ($t_{stat} = 1.9819$, $t_{critical\ (two\text{-}tailed,\ \alpha = 0.05)} = 2.0066$, p value $= 0.0527$) were performed. No significant difference in T-Hg values in GOT sediments analyzed using the two methods was found at the 95% confidence level (Table S6). Nevertheless, DTD-AAS method is less tedious and time-consuming in terms of sample preparation and analysis, thereby reducing human error during preparation steps. Similar to our current study, Panichev and Panicheva (2015) also reported a similar advantage of DTD-AAS over acid-CVAAS for T-Hg analysis in fish tissues.

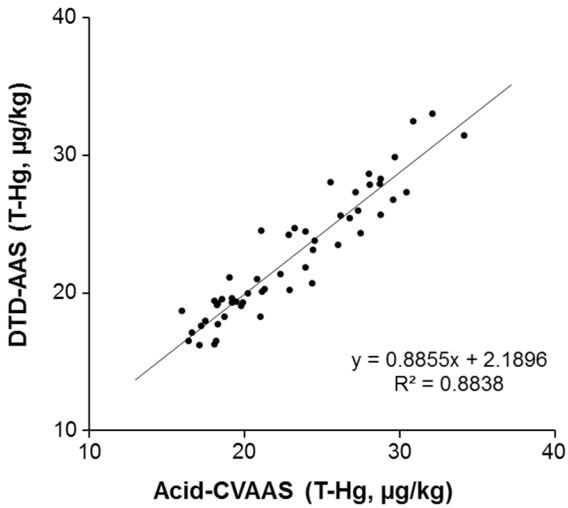

Fig. 2 The T-Hg content (before $CaCO_3$ removal) in 53 representatives of marine sediment samples determined by the DTD-AAS method and the acid-CVAAS method

Sedimentology, geochemical parameters and T-Hg in sediment cores

Sediment in this study was grouped to coarse-grained (63 µm ≤ sand < 2 mm) and fine-grained sediment (size < 63 µm). For all cores except for core 14, more than 98% (w/w) were of fine-grained sediments (Table 1, Fig. S2 in panel a). Core 14, however, was made up of equal parts of coarse-grained and fine-grained sediments. The readily oxidizable organic carbon (ROOC) in the vertical profiles shown in Fig. S2 panel b and the average ROOC content (Table 1) of subsamples from core 14, 22, 29, 35 and BPK were 0.45, 1.53, 0.85, 0.89 and 2.42% (w/w), respectively. The highest $CaCO_3$ contents were observed in core 29 (Table 1) which also exhibited high variation of $CaCO_3$ contents ranging from 16 to 25% (Fig. S2 in panel c). The lowest $CaCO_3$ contents were found in core BPK with a slight increase downcore, from 4% at surface to 8% at bottom. The other cores: core 14, 22 and 35, have an almost constant $CaCO_3$ content throughout the cores with a range of 9–12%.

Concentration of sediment T-Hg in µg/kg dry weight on carbonate-free basis (i.e., normalized by removing $CaCO_3$ content) is reported in Table 1, and T-Hg from DTD-AAS method were selected for further discussion. The depth-averaged T-Hg content in the five sediment cores can be arranged in the following descending order: core BPK > core 14 > core 29 > core 22 > core 35. Observable increases in T-Hg from bottom to surface layers (Fig. S1) were seen in all sediment cores from the middle of GOT. This is consistent with the study of Liu et al. (2016) were reported the same tendency in the sediment cores from the middle part of the gulf. These suggest an increase in T-Hg inputs into the GOT sediment in recent years. For core BPK, the T-Hg content varied within the vertical profile, but the relatively higher T-Hg content at surface layer can still be observed (Fig. S1).

Organic matter and sediment grain size, especially in fine-grained sediment samples, are known for its

Table 1 Descriptive statistics for geochemical variables in core samples, all values were shown as average ± SD in the top row and range in parentheses in the bottom row

Core #	T-Hg by DTD-AAS (μg/kg) carbonate-free basis	T-Hg by acid-CVAAS (μg/kg) carbonate-free basis	ROOC (%w/w) carbonate-free basis	$CaCO_3$ (%w/w)	Sand (%w/w)	Fine grain [%w/w]
14	30.63 ± 3.93 (25.95–36.68)	30.83 ± 4.01 (25.17–37.65)	0.45 ± 0.10 (0.33–0.64)	9.33 ± 0.41 (8.51–10.16)	47.36 ± 6.35 (39.65–57.02)	52.64 ± 6.35 (42.98–60.35)
22	24.85 ± 3.74 (20.90–31.62)	25.44 ± 4.29 (20.13–32.25)	1.53 ± 0.04 (1.45–1.62)	9.71 ± 0.86 (7.84–10.71)	1.04 ± 0.31 (0.43–1.56)	98.96 ± 0.31 (98.44–99.57)
29	28.56 ± 4.67 (21.61–34.05)	29.03 ± 5.77 (19.32–37.85)	0.85 ± 0.09 (0.72–1.05)	19.38 ± 2.78 (15.70–25.16)	1.72 ± 0.66 (0.83–2.79)	98.28 ± 0.66 (97.21–99.17)
35	20.44 ± 1.74 (18.26–23.41)	21.15 ± 2.64 (18.60–27.62)	0.89 ± 0.06 (0.75–1.03)	11.50 ± 0.45 (10.91–12.67)	0.56 ± 0.20 (0.33–0.98)	99.44 ± 0.20 (99.02–99.67)
BPK	48.40 ± 2.13 (44.49–52.76)		– 2.42 ± 0.14 (2.18–2.68)	5.78 ± 0.84 (4.44–7.78)	0.25 ± 0.20 (0.02–0.65)	99.75 ± 0.20 (99.35–99.98)

relation with the concentration of trace/heavy metals in sediment (Covelli et al., 2012; Dou et al., 2013; Kelly & Rudd, 2018; Liu et al., 2016; Meng et al., 2014). These controlling factors influence the distribution of trace/heavy metals including Hg in sediment since they provide strong binding sites to adsorb, complex, and precipitate for metals which are retained within sediment (Chakraborty et al., 2015; Gonzalez-Raymat et al., 2017; Liu et al., 2011). In this study, the correlation between T-Hg content and percentage of fine-grained sediments was not well established due to the fact that most sediment from all of our cores except for core 14 was of entirely fine-grained sediment. Core 14, despite having about half fine-grained sediments in its composition, still did not exhibit such correlation. Very weak positive relationship between T-Hg and ROOC was observed for core 14, 29, 35, and BPK (Fig. S3). In fact, previous studies showed that T-Hg and other heavy metals in the GOT were mainly controlled by both organic matter and fine-grained sediment (Buakaew, 2007; Liu et al., 2016; Sansittisakunlird, 2014). Notably, in core BPK, T-Hg as well as ROOC was highest in concentrations compared with other cores. This indicates that at least for this particular core the organic carbon content is the prime controlling factor of Hg distribution (Fig. S3).

Temporal variation of T-Hg concentration in GOT sediment

^{210}Pb dating and sedimentation rate

Lengths of the sediment cores in this study were less than a meter (Table S1). So, ^{210}Pb dating is a well-suited method for our (likely less than 150 years old) cores as suggested by Barsanti et al. (2020) and Srisuksawad et al. (1997). The vertical profiles of total ^{210}Pb activities vs. depth for 5 sediment cores are shown in Fig. 3. Most cores in this study displayed a typical ^{210}Pb profile characterized by three distinct zones: a surface mixed layer (SML) with uniform or fluctuating ^{210}Pb activities; a middle zone with exponential radioactive decay; and a background zone of consistenly low total ^{210}Pb activity indicating supported ^{210}Pb layer. The decay zone in the middle is used for SAR calculation.

The SML of sediment cores collected from the middle GOT (core 14, 22, 29 and 35) was found down to 6 cm depth, while core BPK has the SML extending down to 18 cm from the sediment surface. The greater thickness of SML in core BPK suggests that sediment in the upper part of the GOT was likely disturbed by the stronger physical and/or

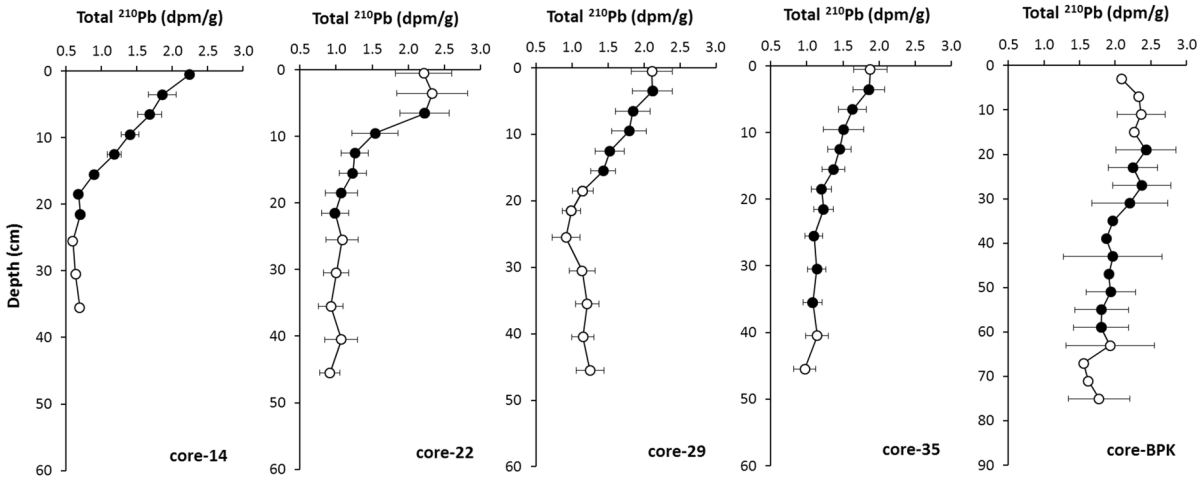

Fig. 3 Depth profiles of total ^{210}Pb activity in the studied cores. Filled circles are points in the decay zone which were used in the calculation of sediment accumulation rates. Empty circles above and below the filled ones are the surface mixed layer and supported ^{210}Pb activity, respectively. Horizontal bars are the uncertainty of the radionuclide measurements

biological processes than the middle GOT. Nevertheless, all sediment cores display the exponentially decrease in total ^{210}Pb activities and is thus suitable for ^{210}Pb dating.

The analyses of ^{210}Pb dating revealed that age span of the sediment cores covered the period in the past for more than 30 years, and up to 140 years (core 22). The information of age and SAR is summarized in Table 2. The SAR of core BPK showed the highest value among others which is not surprising considering that it was collected from the location near the mouth of Bang Pakong River. Previous works reported SAR for the upper GOT to vary in the 0.21–1.14 cm/year range, and SAR near Bang Pakong River mouth was found to be about 0.54–0.78 cm/year (Boonyatumanond et al., 2007; Srisuksawad et al., 1997; Windom et al., 1984), consistent with this study (0.76 cm/year, Table 2).

Core 14 and core 22 were located close to nearshore of Prachuap Khiri Khan and Chumphon provinces (Fig. 1; Table 2), yet they had lower SAR than those of the offshore stations (core 29 and 35). When we compare our calculated SAR values with the SAR contour plot based on SAR data covering entire GOT from Srisuksawad et al. (1997), we found that SAR from core 14 were similar to the contour plot. However, SAR from core 22 (0.15 cm/year, Table 2) was lower than the previous work (0.41 cm/year). Moreover, the offshore stations (core 29 and 35) exhibited the higher SAR (about 0.5 cm/year, Table 2) than previously reported in Srisuksawad et al. (1997) (0.2 cm/year, Fig. 1). Location of sediment cores and coastal currents likely attributed to such disparity. The strong seasonal coastal currents in southwestern GOT from which core 14 and 22 were collected might hamper sediment accumulation in this area. In contrast, the slow velocity of geostrophic

Table 2 Age and sediment accumulation rate (SAR) in the five sediment cores in this study

Core #	Surface mixed layer (cm)	Section (cm)	Age span (A.D.)	Range (year)	SAR (cm/year)
14	0	0–22	1922–2016	94	0.22
22	0–6	0–22	1875–2015	140	0.15
29	0–3	0–16	1983–2017	34	0.45
35	0–3	0–36	1948–2017	69	0.50
BPK	0–18	0–60	1942–2016	74	0.76

current occurred at which core 29 and 35 are situated may boost the deposition of new sediment (Buranapratheprat et al., 2016; Sojisuporn et al., 2009).

Temporal variation of T-Hg in the GOT

The start of the industrialized period in Thailand dated back to 1961 when the nation's First Economic Development Plan of Thailand was launched. ^{210}Pb sediment dating coupled with the CFCS model provided accurate sediment ages up to 150 years, allowing us to study the medium-term pollution history in the GOT. The T-Hg contents in the GOT sediment over 100 years ago were constructed from the older sediment layers to the last bottom layers with an extrapolated estimation based on SAR of each core and illustrated in Fig. 4. Concentration of T-Hg in all sediment cores showed a gradual increase with age span back to twentieth century, while in core 22 can be dated back to the time before then.

Core BPK in the upper GOT houses the T-Hg polluted sediment impacted by land-based sources. Three chorological segments with varying T-Hg contents were observed. The first was the period before the 1960s when T-Hg was slowly increasing from 44.49 to 50.83 µg/kg. The second was defined as the period between the 1960s until 2005 when there was a decrease in T-Hg concentration from 50.83 to 46.07 µg/kg. Meanwhile, the third period spanned between 2005 and the present and this was marked by a rapid increase in T-Hg concentration from 46.07 to 52.76 µg/kg. This temporal changes in BPK core similarly reflected the global trend of Hg production, consumption and emission patterns during year 1950 to 2010 where peaked at 1970 and declined until 2000 (Horowitz et al., 2014; Streets et al., 2019). The unusually high T-Hg content in BPK core after 2005 might be related to the bunker oil spill accident in 2008 at a shipyard close to Chao Phraya River mouth not too far from where this core was collected. Many literatures suggested that fossil fuels (i.e., coal, crude oil, and natural gas) contain high T-Hg content (DeLaune et al., 2008; Jian et al., 2019; Tang et al., 2019; Wilhelm, 2001; Wilhelm & Bloom, 2000; Wong et al., 2006).

Unlike global Hg production, consumption and emission patterns (Horowitz et al., 2014; Streets et al., 2019), the increase in the accumulation of T-Hg was apparent in all 4 cores in the middle of the GOT (Fig. 4). At the bottom of each core (core 14, 22, and 35), T-Hg concentration is relatively uniform at what we could consider as the background levels for the study area, which are around 20–25 µg/kg (Fig. 4 and S1). Before the industrialized period began (1960s), concentration of T-Hg in nearshore stations (core 14 and 22) was markedly higher than those from the offshore stations (core 29 and core 35), suggesting that primary source of T-Hg accumulated in sediment was land-based. The southern part of Thailand is rich in minerals, and inland-artisanal mining has been recorded to start over 100 years ago (information from http://www.dmr.go.th, the Department of

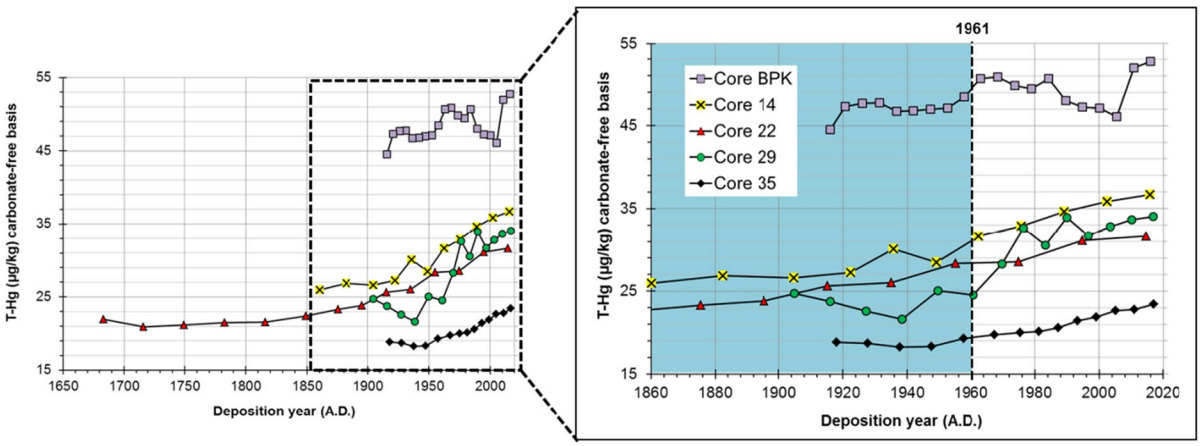

Fig. 4 Historical T-Hg contents from the five sediment cores in this study. Deposition years were based on ^{210}Pb dating, and 1961 is marked as the start of industrial period in Thailand (i.e., the commencement of the nation's First Economic Development Plan)

Mineral Resources of Thailand). This mining activity accelerates weathering and erosion while at the same time stripping the surface soil. Consequently, toxic substances from mining operations may be discharged and collected in the runoff from mining site and ultimate flowed into the sea. Noticeably, T-Hg began to increase gradually from year 1922, 1816, 1938, and 1948 in core 14, 22, 29 and 35, respectively.

Due to human activities on land, T-Hg content in nearshore sediments usually displays higher T-Hg than offshore sediments (Liu et al., 2011, 2017; Meng et al., 2014; Yang et al., 2015). The present study, however, found that the offshore core 29 had a slightly higher Hg content (average 28.56 ± 4.67 µg/kg) than the nearshore core 22 (average 24.85 ± 3.74 µg/kg). This implies additional marine-based sources of Hg that may be related to offshore-petroleum exploration/production activities (DMF, 2018) and frequent accidental oil spills within the gulf (Wattayakorn, 2012). Coincidentally, the escalating trend of T-Hg in the sediment core in the middle of GOT (core 29) was linked with the period where to the first national development plan were initiated in 1961 and the petroleum exploration/production began in 1968 (DMF, 2018). It can be seen that T-Hg in core 29 increased rapidly after 1960s (Fig. 4 and Table S7). Moreover, the T-Hg distribution in the surface sediment collected after 2000 in the GOT also indicated the higher T-Hg contents in the middle GOT than other areas in the western GOT (Buakaew, 2007; Liu et al., 2016; Sansittisakunlird, 2014; SEAFDEC, 2013). Similar increasing pattern was also found in sediment cores collected from Yellow and East China Seas (Kim et al., 2018) and coastal ponds of St. Thomas in the U.S. Virgin Islands (Benoit, 2018) where reported the adjacent local Hg source.

T-Hg contaminated status in the GOT sediment and its possible sources

Our study and previous works (Buakaew, 2007; Liu et al., 2016; Sansittisakunlird, 2014; SEAFDEC, 2013; Thongra-ar et al., 2008), T-Hg values in the GOT sediment (Fig. 5) were lower than the following the guideline values of Thailand's Sediment Quality Guidelines (Pollution Control Department of Thailand, 2015) and other countries (Buchman, 2008; Canadian Council of Ministers of the Environment, 1999; Chapman et al., 1999). The exception was for the samples from estuarine sediment in the Chao Phraya River whose average T-Hg concentrations were at 396 µg/kg (Sirirattanachai, 2001).

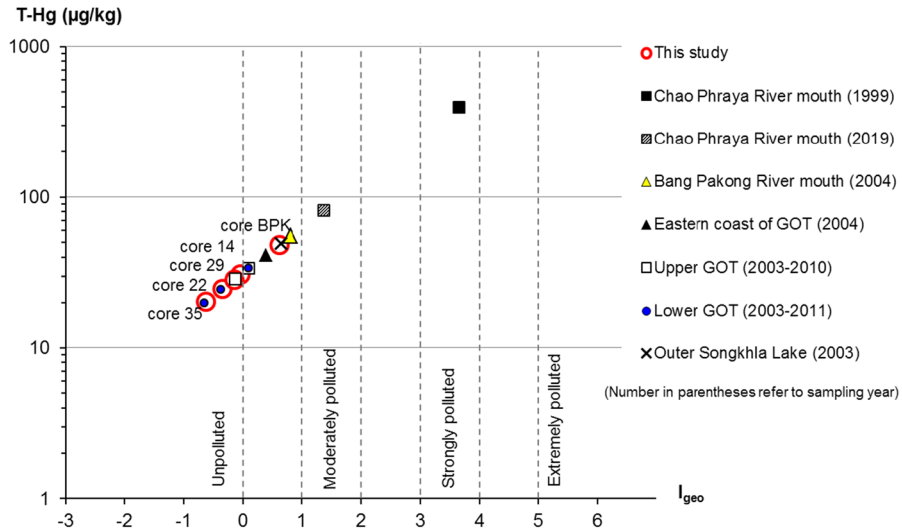

Fig. 5 T-Hg concentrations and I_{geo} index values in the Gulf of Thailand (GOT) from this study and our investigation on Chao Phraya River (Sompongchaiyakul et al., unpublished data) and other previous works from Chao Phraya (Sirirattanachai, 2001), Bang Pakong River and Eastern coast of GOT (Thongra-ar et al., 2008), Songkhla Lake (Sompongchaiyakul & Sirinawin, 2007), Upper GOT (Buakaew, 2007; Sansittisakunlird, 2014), and Lower GOT (Buakaew, 2007; Liu et al., 2016; SEAFDEC, 2013)

Though this T-Hg in the estuarine sediment exceeded all stated in the above guidelines, it was orders of magnitude lower than no-observed-effect concentrations (for field site investigation at 22 mg/kg) that was suggested in Conder et al. (2015) study. In addition, we have recently re-investigated surface sediment in the Chao Phraya River mouth in 2019 and the average T-Hg concentrations was declined to 82 µg/kg (Sompongchaiyakul et al., unpublished data). The reduction in T-Hg in sediment may likely link to the re-processing to mercury free in chlor-alkali industrial plants.

Geoaccumulation index (I_{geo}) proposed by Müller (1969) and widely used in various heavy metal studies (Liu et al., 2016; Wang et al., 2018) was adopted to evaluate the degree of T-Hg contamination in our sediment samples. The I_{geo} was classified from class 1 ($I_{geo} \leq 0$) to class 6 ($I_{geo} > 5$). The highest class corresponded to at least a 100-fold enrichment above the background value (Liu et al., 2016; Zhuang & Gao, 2015). The I_{geo} is calculated by the following equation:

$$I_{geo} = \log_2 \left[C_n / \left(1.5 \times B_n \right) \right]$$

where C_n is the measured Hg concentration; B_n is background Hg concentration.

Generally, an average shale value (400 µg/kg) was applied for background Hg concentration (Turekian and Wedepohl (1961). Applying this background Hg concentration in the study, the reported $I_{geo} < 0$ for all sediment in the GOT showing that all the GOT sediments were classified in an unpolluted status. However, the T-Hg concentrations in all 5 sediment cores were about 10 times lower than the average shale concentration. Thus, we have proposed to use the local B_n value obtaining from the sediment cores data instead to illustrate the transition change of T-Hg concentration in the GOT sediment over a period of time. The T-Hg background adopted in this study was 21 µg/kg or an average T-Hg background concentration from core 22 where located to nearshore and was the oldest core from dating. By using the local I_{geo} index, sediment in this study was classified as an unpolluted to moderately polluted status (Fig. 5). Notably, T-Hg concentration and I_{geo} tend to decrease from the river mouth to coastal sediments and from the upper GOT to the lower GOT, respectively (Fig. 5). This indicated the influences of the land-based sources entering T-Hg into the GOT; including weathering and erosion of coastal and inland sediment, untreated municipal waste and sewage and river runoff (Cheevaporn & Menasveta, 2003), industrial estates (Thongra-ar et al., 2008), gold mining (Nakbanpote et al., 2018; Pataranawat et al., 2007), petroleum product usages (Boonyatumanond et al., 2007), and onshore petroleum sources (DMF, 2018).

Conclusion

Previous studies examined T-Hg in the GOT sediment using a classical acid digestion or acid-CVAAS method. This study, the alternative DTD-AAS method, was used and compared. Results showed good agreement between both methods with no significant difference of T-Hg at 95% confidence level for 53 marine sediment core samples (core 14, 22, 29, and 35) collected from the middle of the western GOT. The ^{210}Pb method based on CFCS model was used to study recent sediment chronologies and sediment accumulation rate (SAR) in those sediment cores. Cores 14, 22, 29, and 35 exhibited age spans covering the 1940s to 2016, and SAR ranging from 0.2 to 0.5 cm/year. While, core BPK collected from Bang Pakong River mouth showed the highest SAR at about 0.8 cm/year with similar age spans.

Core BPK were likely be most impacted by Hg from land-based sources with the highest concentration in this study at 52.76 µg/kg. Average T-Hg contents decreased as following order from core BPK > core 14 > core 29 > core 22 > core 35. Vertical profiles vs. time illustrated clearly increasing trend of T-Hg, especially the cores in the middle GOT. The increasing rates of T-Hg can be observed after 1960s where is the period of industrialization begun in Thailand. Before which, land-based sources were the most significant sources of Hg in core BPK and nearshore stations (core 14 and 22). Remarkably, the increase in T-Hg in offshore stations core 29 after 1961 was likely a signal from marine-based sources associated with offshore-petroleum exploration/production activities initiated a few years after the beginning of the nation's First Economic Development Plan of Thailand. In this study, the status of T-Hg in the GOT sediment can be classified as an unpolluted to moderately polluted status determined by the I_{geo}

index using the local background concentration from sediment core 22 (an average T-Hg at 21 µg/kg).

Acknowledgements We would like to thank SEAFDEC for organizing the 2018 research cruise and facilitating sediment core sampling. We are indebted to the captains and crew of M.V. SEAFDEC-2 and M.V. Kasetsart-1 for their tremendous help during the sampling. T. Ubonyaem was supported by Science Achievement Scholarship of Thailand (SAST). Thanks to COAX Group Corporation Ltd. for providing the assistance and the usage of the direct thermal decomposition mercury analyzer MA-3000 (NIC). Funding of this research was granted by the 90th Anniversary of Chulalongkorn University Fund (Ratchadaphiseksomphot Endowment Fund). ^{210}Pb dating analysis was conducted at the Department of Nuclear Engineering, Faculty of Engineering, Chulalongkorn University with helps from Professor Supitcha Chanyotha, Dr. Rawiwan Kritsananuwat, Ampika Jawana, and Prathan Mirattanaphai. Thanks to Chanakarn Suphanthong and Pilartrut Sing-in for their laboratory assistance.

Author contribution All authors contributed significantly toward the makeup of the paper. Conceptualization, methodology, investigation, writing—original draft, review & editing, and data curation, were performed by Tanakorn Ubonyaem. Sujaree Bureekul and Chawalit Charoenpong contributed to conceptualization, methodology, supervision, writing—review & editing. Pontipa Luadnakrob contributed to resources and investigation. Penjai Sompongchaiyakul contributed to conceptualization, methodology, resources, funding acquisition, supervision, writing— review & editing and project administration.

Funding Funding of this research was provided by the 90th Anniversary of Chulalongkorn University Fund (Ratchadaphiseksomphot Endowment Fund).

Declarations

Conflict of interest The authors declare that they have no known competing financial or non-financial interests that could have appeared to influence the work reported in this paper.

References

Agah, H., Elskens, M., Fatemi, S. M. R., Owfi, F., Baeyens, W., & Leermakers, M. (2009). Mercury speciation in the Persian Gulf sediments. *Environmental Monitoring and Assessment, 157*(1), 363–373. https://doi.org/10.1007/s10661-008-0541-x

Barsanti, M., Garcia-Tenorio, R., Schirone, A., Rozmaric, M., Ruiz-Fernández, A. C., Sanchez-Cabeza, J. A., Delbono, I., Conte, F., De Oliveira Godoy, J. M., Heijnis, H., Eriksson, M., Hatje, V., Laissaoui, A., Nguyen, H. Q., Okuku, E., Al-Rousan, S. A., Uddin, S., Yii, M. W., & Osvath, I. (2020). Challenges and limitations of the ^{210}Pb sediment dating method: Results from an IAEA modelling interlaboratory comparison exercise. *Quaternary Geochronology, 59*, 101093. https://doi.org/10.1016/j.quageo.2020.101093

Begy, R. C., Dumitru, O. A., Simon, H., & Steopoaie, I. (2015). An improved procedure for the determination of 210Po by alpha spectrometry in sediments samples from Danube Delta. *Journal of Radioanalytical and Nuclear Chemistry, 303*(3), 2553–2557. https://doi.org/10.1007/s10967-014-3703-z

Benoit, G. (2018). Mercury in dated sediment cores from coastal ponds of St Thomas, USVI. *Marine Pollution Bulletin, 126*, 535–539. https://doi.org/10.1016/j.marpolbul.2017.09.056

Boonyatumanond, R., Wattayakorn, G., Amano, A., Inouchi, Y., & Takada, H. (2007). Reconstruction of pollution history of organic contaminants in the upper Gulf of Thailand by using sediment cores: First report from Tropical Asia Core (TACO) project. *Marine Pollution Bulletin, 54*(5), 554–565. https://doi.org/10.1016/j.marpolbul.2006.12.007

Braune, B., Chételat, J., Amyot, M., Brown, T., Clayden, M., Evans, M., Fisk, A., Gaden, A., Girard, C., Hare, A., Kirk, J., Lehnherr, I., Letcher, R., Loseto, L., Macdonald, R., Mann, E., McMeans, B., Muir, D., O'Driscoll, N., … Stern, G. (2015). Mercury in the marine environment of the Canadian Arctic: Review of recent findings. *Science of the Total Environment, 509–510*, 67–90. https://doi.org/10.1016/j.scitotenv.2014.05.133

Bruel, R., & Sabatier, P. (2020). serac: An R package for ShortlivEd RAdionuclide chronology of recent sediment cores. *Journal of Environmental Radioactivity, 225*, 106449. https://doi.org/10.1016/j.jenvrad.2020.106449

Buakaew, S. (2007). Contamination of mercury in surface sediment in the Gulf of Thailand. (Master's thesis). Chulalongkorn University, http://cuir.car.chula.ac.th/handle/123456789/14325.

Buchman, M. F. (2008). NOAA Screening quick reference tables (SquiRTs). https://response.restoration.noaa.gov/cpr/sediment/squirt/squirt.html.

Buranapratheprat, A., Luadnakrob, P., Yanagi, T., Morimoto, A., & Qiao, F. (2016). The modification of water column conditions in the Gulf of Thailand by the influences of the South China Sea and monsoonal winds. *Continental Shelf Research, 118*, 100–110. https://doi.org/10.1016/j.csr.2016.02.016

Canadian Council of Ministers of the Environment. (1999). Canadian sediment quality guidelines for the protection of aquatic life: Mercury. https://ccme.ca/en/current-activities/canadian-environmental-quality-guidelines.

Chakraborty, P., Sarkar, A., Vudamala, K., Naik, R., & Nath, B. N. (2015). Organic matter—A key factor in controlling mercury distribution in estuarine sediment. *Marine Chemistry, 173*, 302–309. https://doi.org/10.1016/j.marchem.2014.10.005

Chapman, P. M., Allard, P. J., & Vigers, G. A. (1999). Development of sediment quality values for Hong Kong special administrative region: A possible model for other jurisdictions. *Marine Pollution Bulletin, 38*(3), 161–169. https://doi.org/10.1016/S0025-326X(98)00162-3

Charoensawadpong, P., Chatwarodom, P., Manit, P., Atibodhi, N., Yongmanitchai, M., Hayook, C., Sujijantararat, K., &

Suwanvesh, K. (2018). *Unlocking field potential from high mercury wells: New opportunities, challenges and solutions*. Paper presented at the Offshore Technology Conference Asia. https://doi.org/10.4043/28524-MS

Cheevaporn, V., & Menasveta, P. (2003). Water pollution and habitat degradation in the Gulf of Thailand. *Marine Pollution Bulletin, 47*(1–6), 43–51. https://doi.org/10.1016/S0025-326X(03)00101-2

Cizdziel, J. V., Hinners, T. A., & Heithmar, E. M. (2002). Determination of total mercury in fish tissues using combustion atomic absorption spectrometry with gold amalgamation. *Water, Air, and Soil Pollution, 135*(1), 355–370. https://doi.org/10.1023/A:1014798012212

Conder, J. M., Fuchsman, P. C., Grover, M. M., Magar, V. S., & Henning, M. H. (2015). Critical review of mercury sediment quality values for the protection of benthic invertebrates. *Environmental Toxicology and Chemistry, 34*(1), 6–21. https://doi.org/10.1002/etc.2769

Covelli, S., Protopsalti, I., Acquavita, A., Sperle, M., Bonardi, M., & Emili, A. (2012). Spatial variation, speciation and sedimentary records of mercury in the Guanabara Bay (Rio de Janeiro, Brazil). *Continental Shelf Research, 35*, 29–42. https://doi.org/10.1016/j.csr.2011.12.003

DeLaune, R. D., Devai, I., Hou, A., & Jugsujinda, A. (2008). Total and methyl Hg in sediment adjacent to offshore platforms of the Gulf of Mexico. *Soil and Sediment Contamination: An International Journal, 17*(2), 98–106. https://doi.org/10.1080/15320380701870153

DMF. (2018). ANNUAL REPORT 2018. https://dmf.go.th/public/list/data/index/menu/668

Dou, Y., Li, J., Zhao, J., Hu, B., & Yang, S. (2013). Distribution, enrichment and source of heavy metals in surface sediments of the eastern Beibu Bay, South China Sea. *Marine Pollution Bulletin, 67*(1), 137–145. https://doi.org/10.1016/j.marpolbul.2012.11.022

Elezz, A. A., Mustafa Hassan, H., Abdulla Alsaadi, H., Easa, A., Al-Meer, S., Elsaid, K., Ghouri, Z. K., & Abdala, A. (2018). Validation of total mercury in marine sediment and biological samples, using cold vapour atomic absorption spectrometry. *Methods and Protocols, 1*(3), 31. https://doi.org/10.3390/mps1030031

Fitzgerald, W. F., Lamborg, C. H., & Hammerschmidt, C. R. (2007). Marine biogeochemical cycling of mercury. *Chemical Reviews, 107*(2), 641–662. https://doi.org/10.1021/cr050353m

Franklin, R. L., Bevilacqua, J. E., & Favaro, D. I. T. (2012). Organic and total mercury determination in sediments by cold vapor atomic absorption spectrometry: Methodology validation and uncertainty measurements. *Quím. Nova, 35*, 45–50. https://doi.org/10.1590/S0100-40422012000100009

Gilmour, C., Bell, J. T., Soren, A. B., Riedel, G., Riedel, G., Kopec, A. D., & Bodaly, R. A. (2018). Distribution and biogeochemical controls on net methylmercury production in Penobscot River marshes and sediment. *Science of the Total Environment, 640–641*, 555–569. https://doi.org/10.1016/j.scitotenv.2018.05.276

Gonzalez-Raymat, H., Liu, G., Liriano, C., Li, Y., Yin, Y., Shi, J., Jiang, G., & Cai, Y. (2017). Elemental mercury: Its unique properties affect its behavior and fate in the environment. *Environmental Pollution, 229*, 69–86. https://doi.org/10.1016/j.envpol.2017.04.101

Gworek, B., Bemowska-Kałabun, O., Kijeńska, M., & Wrzosek-Jakubowska, J. (2016). Mercury in marine and oceanic waters—A review. *Water, Air, & Soil Pollution, 227*(10), 371. https://doi.org/10.1007/s11270-016-3060-3

Homira, A., S. Mohamad Reza, F., Mehdinia, A., & Ahmad, S. (2009). Determining total mercury in samples from the Persian Gulf and the Caspian Sea: Comparison of dry ash and wet extraction mothods. *Journal of the Persian Gulf (Marine Science), 2*(4), 11–18. http://jpg.inio.ac.ir/article-1-22-fa.html

Horowitz, H. M., Jacob, D. J., Amos, H. M., Streets, D. G., & Sunderland, E. M. (2014). Historical mercury releases from commercial products: Global environmental implications. *Environmental Science & Technology, 48*(17), 10242–10250. https://doi.org/10.1021/es501337j

Huber, J., & Leopold, K. (2016). Nanomaterial-based strategies for enhanced mercury trace analysis in environmental and drinking waters. *TrAC Trends in Analytical Chemistry, 80*, 280–292. https://doi.org/10.1016/j.trac.2015.09.007

Issaro, N., Abi-Ghanem, C., & Bermond, A. (2009). Fractionation studies of mercury in soils and sediments: A review of the chemical reagents used for mercury extraction. *Analytica Chimica Acta, 631*(1), 1–12. https://doi.org/10.1016/j.aca.2008.10.020

Jian, L., Zhongxi, H., Qituan, Y., Shuying, W., & Shouguo, G. (2019). Distribution and genesis of mercury in natural gas of large coal derived gas fields in China. *Petroleum Exploration and Development, 46*(3), 463–470. https://doi.org/10.1016/S1876-3804(19)60027-3

Kan, M., Willie, S. N., Scriver, C., & Sturgeon, R. E. (2006). Determination of total mercury in biological samples using flow injection CVAAS following tissue solubilization in formic acid. *Talanta, 68*(4), 1259–1263. https://doi.org/10.1016/j.talanta.2005.07.027

Kelly, C. A., & Rudd, J. W. M. (2018). Transport of mercury on the finest particles results in high sediment concentrations in the absence of significant ongoing sources. *Science of the Total Environment, 637–638*, 1471–1479. https://doi.org/10.1016/j.scitotenv.2018.04.234

Kim, J., Lim, D., Jung, D., Kang, J., Jung, H., Woo, H., Jeong, K., & Xu, Z. (2018). Sedimentary mercury (Hg) in the marginal seas adjacent to Chinese high-Hg emissions: Source-to-sink, mass inventory, and accumulation history. *Marine Pollution Bulletin, 128*, 428–437. https://doi.org/10.1016/j.marpolbul.2018.01.058

Leng, G., Feng, L., Li, S.-B., Qian, S., & Dan, D.-Z. (2013). Determination of mercury (Hg) in sediment by a sequential injection (SI) system with cold vapor generation atomic fluorescence spectrometry (CVAFS) detection after a rapid and mild microwave-assisted digestion. *Environmental Forensics, 14*(1), 9–15. https://doi.org/10.1080/15275922.2012.729003

Liu, S., Shi, X., Liu, Y., Zhu, Z., Yang, G., Zhu, A., & Gao, J. (2011). Concentration distribution and assessment of heavy metals in sediments of mud area from inner continental shelf of the East China Sea. *Environmental Earth Sciences, 64*(2), 567–579. https://doi.org/10.1007/s12665-011-0941-z

Liu, S., Shi, X., Yang, G., Khokiattiwong, S., & Kornkanitnan, N. (2016). Concentration distribution and assessment of heavy metals in the surface sediments of the western Gulf of Thailand. *Environmental Earth Sciences, 75*(4), 346. https://doi.org/10.1007/s12665-016-5422-y

Liu, W., Hu, L., Lin, T., Li, Y., & Guo, Z. (2017). Distribution and mass inventory of mercury in sediment from the Yangtze River estuarine-inner shelf of the East China Sea. *Continental Shelf Research, 132*, 29–37. https://doi.org/10.1016/j.csr.2016.11.004

Loring, D. H., & Rantala, R. T. T. (1992). Manual for the geochemical analyses of marine sediments and suspended particulate matter. *Earth-Science Reviews, 32*(4), 235–283. https://doi.org/10.1016/0012-8252(92)90001-A

Meng, M., Shi, J.-B., Yun, Z.-J., Zhao, Z.-S., Li, H.-J., Gu, Y.-X., Shao, J.-J., Chen, B.-W., Li, X.-D., & Jiang, G.-B. (2014). Distribution of mercury in coastal marine sediments of China: Sources and transport. *Marine Pollution Bulletin, 88*(1), 347–353. https://doi.org/10.1016/j.marpolbul.2014.08.028

Müller, G. (1969). Index of geoaccumulation in sediments of the Rhine River. *GeoJournal, 2*, 108–118.

Nakbanpote, W., Prasad, M. N. V., Mongkhonsin, B., Panitlertumpai, N., Munjit, R., & Rattanapolsan, L. (2018). Chapter 33—Strategies for rehabilitation of mine waste/leachate in Thailand. In M. N. V. Prasad, P. J. d. C. Favas, & S. K. Maiti (Eds.), *Bio-geotechnologies for mine site rehabilitation* (pp. 617–643). Elsevier.

Panichev, N. A., & Panicheva, S. E. (2015). Determination of total mercury in fish and sea products by direct thermal decomposition atomic absorption spectrometry. *Food Chemistry, 166*, 432–441. https://doi.org/10.1016/j.foodchem.2014.06.032

Pataranawat, P., Parkpian, P., Polprasert, C., Delaune, R. D., & Jugsujinda, A. (2007). Mercury emission and distribution: Potential environmental risks at a small-scale gold mining operation, Phichit Province, Thailand. *Journal of Environmental Science and Health, Part A, 42*(8), 1081–1093. https://doi.org/10.1080/10934520701418573

Pollution Control Department of Thailand. (2015). *Announcement of the pollution control department "establish criteria for quality of coastal sediment" (in Thai).*

Pongsiri, N. (1997). *Thailand's initiatives on mercury*. Paper presented at the SPE Asia Pacific Oil and Gas Conference and Exhibition. https://doi.org/10.2118/38087-MS

Sansittisakunlird, B. (2014). *Spatial contamination and baseline of mercury in surface sediment of the Gulf of Thailand.* (Master's thesis). Chulalongkorn University (in Thai), http://cuir.car.chula.ac.th/handle/123456789/44533

SEAFDEC. (2013). *Research results of the survey of fisheries resources and marine environment in the central Gulf of Thailand By M.V.SEAFDEC Year 2013 (in Thai).* http://hdl.handle.net/20.500.12067/678

Shoham-Frider, E., Azran, S., & Kress, N. (2012). Mercury speciation and total organic carbon in marine sediments along the Mediterranean coast of Israel. *Archives of Environmental Contamination and Toxicology, 63*(4), 495–502. https://doi.org/10.1007/s00244-012-9803-2

Sirirattanachai, S. (2001). *Geochemistry of mercury in the Chao Phraya River estuary.* (Doctoral dissertation). Chulalongkorn University. http://cuir.car.chula.ac.th/handle/123456789/9401

Sojisuporn, P., Morimoto, A., & Yanagi, T. (2009). *Seasonal variation of sea surface current in the Gulf of Thailand.* Paper presented at the 4th JSPS-VAST Joint Seminar on 'Coastal Marine Science', Hai Phong, Viet Nam, 26–28 October 2009.

Sompongchaiyakul, P. (1989). *Analysis of chemical species for trace metals in near-shore sediment by sequential leaching method.* (Master's thesis). Chulalongkorn University. http://cuir.car.chula.ac.th/handle/123456789/31454

Sompongchaiyakul, P., & Sirinawin, W. (2007). Arsenic, chromium and mercury in surface sediment of Songkhla Lake System, Thailand. *Asian Journal of Water, Environment and Pollution, 4*, 17–24.

Srisuksawad, K., Porntepkasemsan, B., Nouchpramool, S., Yamkate, P., Carpenter, R. O. Y., Peterson, M. L., & Hamilton, T. (1997). Radionuclide activities, geochemistry, and accumulation rates of sediments in the Gulf of Thailand. *Continental Shelf Research, 17*(8), 925–965. https://doi.org/10.1016/S0278-4343(96)00065-9

Streets, D. G., Horowitz, H. M., Lu, Z., Levin, L., Thackray, C. P., & Sunderland, E. M. (2019). Five hundred years of anthropogenic mercury: spatial and temporal release profiles*. *Environmental Research Letters, 14*(8), 084004. https://doi.org/10.1088/1748-9326/ab281f

Tang, S., Zhou, Y., Yao, X., Feng, X., Li, Z., Wu, G., & Guangyou, Z. (2019). The mercury isotope signatures of coalbed gas and oil-type gas: Implications for the origins of the gases. *Applied Geochemistry, 109*, 104415. https://doi.org/10.1016/j.apgeochem.2019.104415

Thongra-ar, W., Musika, C., Wongsudawan, W., & Munhapol, A. (2008). Heavy metals contamination in sediments along the Eastern Coast of the Gulf of Thailand. *EnvironmentAsia, 1*, 37–45. https://doi.org/10.14456/ea.2008.5

Turekian, K. K., & Wedepohl, K. H. (1961). Distribution of the elements in some major units of the earth's crust. *GSA Bulletin, 72*(2), 175–192. https://doi.org/10.1130/0016-7606(1961)72[175:DOTEIS]2.0.CO;2

US EPA. (1994). *"Method 245.1: Determination of mercury in water by cold vapor atomic absorption spectrometry." Revision 3.0. Cincinnati, OH*. https://www.epa.gov/esam/epa-method-2451-determination-mercury-water-cold-vapor-atomic-absorption-spectrometry

US EPA. (1998). *"Method 7473 (SW-846): Mercury in solids and solutions by thermal decomposition, amalgamation, and atomic absorption spectrophotometry".* https://www.epa.gov/esam/epa-method-7473-sw-846-mercury-solids-and-solutions-thermal-decomposition-amalgamation-and

US EPA. (2001). *Appendix to Method 1631: Total mercury in tissue, sludge, sediment, and soil by acid digestion and BrCl oxidation*. https://nepis.epa.gov/Exe/ZyPURL.cgi?Dockey=40001F6A.txt

US EPA. (2002). *Method 1631, Revision E: Mercury in water by oxidation, purge and trap, and cold vapor atomic fluorescence spectrometry*. https://nepis.epa.gov/Exe/ZyPURL.cgi?Dockey=P1008IW8.txt

Wang, C.-C., Pan, D.-W., Han, H.-T., & Hu, X.-P. (2018). Distribution and contamination assessment of arsenic and mercury in surface sediments from the intertidal zone of Yantai Sishili Bay, China. *Human and Ecological Risk*

Assessment: An International Journal, 24(8), 2024–2035. https://doi.org/10.1080/10807039.2018.1436435

Wang, S., Jia, Y., Wang, S., Wang, X., Wang, H., Zhao, Z., & Liu, B. (2009). Total mercury and monomethylmercury in water, sediments, and hydrophytes from the rivers, estuary, and bay along the Bohai Sea coast, northeastern China. *Applied Geochemistry, 24*(9), 1702–1711. https://doi.org/10.1016/j.apgeochem.2009.04.037

Wattayakorn, G. (2012). Petroleum pollution in the Gulf of Thailand: A historical review. *Coastal Marine Science, 35*(1), 234–245. https://doi.org/10.15083/00040658

Wilhelm, S. M. (2001). Estimate of mercury emissions to the atmosphere from petroleum. *Environmental Science & Technology, 35*(24), 4704–4710. https://doi.org/10.1021/es001804h

Wilhelm, S. M., & Bloom, N. (2000). Mercury in petroleum. *Fuel Processing Technology, 63*(1), 1–27. https://doi.org/10.1016/S0378-3820(99)00068-5

Windom, H. L., Silpipat, S., Chanpongsang, A., Smith, R. G., & Hungspreugs, M. (1984). Trace metal composition of and accumulation rates of sediments in the Upper Gulf of Thailand. *Estuarine, Coastal and Shelf Science, 19*(2), 133–142. https://doi.org/10.1016/0272-7714(84)90060-X

Wong, C. S. C., Duzgoren-Aydin, N. S., Aydin, A., & Wong, M. H. (2006). Sources and trends of environmental mercury emissions in Asia. *Science of the Total Environment, 368*(2), 649–662. https://doi.org/10.1016/j.scitotenv.2005.11.024

Yang, X., Yuan, X., Zhang, A., Mao, Y., Li, Q., Zong, H., Wang, L., & Li, X. (2015). Spatial distribution and sources of heavy metals and petroleum hydrocarbon in the sand flats of Shuangtaizi Estuary, Bohai Sea of China. *Marine Pollution Bulletin, 95*(1), 503–512. https://doi.org/10.1016/j.marpolbul.2015.02.042

Yeager, K. M., Schwehr, K. A., Schindler, K. J., & Santschi, P. H. (2018). Sediment accumulation and mixing in the Penobscot River and estuary, Maine. *Science of the Total Environment, 635*, 228–239. https://doi.org/10.1016/j.scitotenv.2018.04.026

Zaborska, A., Carroll, J., Papucci, C., & Pempkowiak, J. (2007). Intercomparison of alpha and gamma spectrometry techniques used in ^{210}Pb geochronology. *Journal of Environmental Radioactivity, 93*(1), 38–50. https://doi.org/10.1016/j.jenvrad.2006.11.007

Zhao, L., Wang, R., Zhang, C., Yin, D., Yang, S., & Huang, X. (2019). Geochemical controls on the distribution of mercury and methylmercury in sediments of the coastal East China Sea. *Science of the Total Environment, 667*, 133–141. https://doi.org/10.1016/j.scitotenv.2019.02.334

Zhu, W., Song, Y., Adediran, G. A., Jiang, T., Reis, A. T., Pereira, E., Skyllberg, U., & Björn, E. (2018). Mercury transformations in resuspended contaminated sediment controlled by redox conditions, chemical speciation and sources of organic matter. *Geochimica Et Cosmochimica Acta, 220*, 158–179. https://doi.org/10.1016/j.gca.2017.09.045

Zhuang, W., & Gao, X. (2015). Distributions, sources and ecological risk assessment of arsenic and mercury in the surface sediments of the southwestern coastal Laizhou Bay, Bohai Sea. *Marine Pollution Bulletin, 99*(1), 320–327. https://doi.org/10.1016/j.marpolbul.2015.07.037

Supplementary Information

Preindustrial levels and temporal enrichment trends of mercury in sediment cores from the Gulf of Thailand

Journal: Environmental Geochemistry and Health

Tanakorn Ubonyaem[a], Sujaree Bureekul[a], Chawalit Charoenpong[a], Pontipa Luadnakrob[b], Penjai Sompongchaiyakul[a,*]

[a]Department of Marine Science, Faculty of Science, Chulalongkorn University, Bangkok, Thailand, 10330.

[b]Southeast Asian Fisheries Development Center, Training Department, Samut Prakan, Thailand, 10290.

*Corresponding Author; Penjai Sompongchaiyakul

Phone Number: +66 22 18 5408

E-mail: penjai.s@chula.ac.th

Table S1 Sampling detail of the five sediment cores used in this study

Core #	Longitude (^{o}E)	Latitude (^{o}N)	Water depth (m)	Sampling date	Core length (cm)
14	99.7570	11.2531	42.0	26 Aug 2018	40
22	99.6737	10.3726	46.8	02 Sep 2018	51
29	101.0878	9.7761	68.0	29 Aug 2018	50
35	101.0893	8.7183	53.0	08 Sep 2018	51
BPK	100.8522	13.3802	10.8	16 Jan 2020	80

Table S2 Comparison of analytical performance between DTD-AAS and acid-CVAAS methods

Parameter	DTD-AAS (ng of Hg)	Acid-CVAAS	
		µg/L	ng of Hg*
Linear working range	0 – 10 (low range) 0 – 1500 (high range)	0.1 – 10	0.05 – 5
Instrument-LOD	0.001	0.010	0.005
Instrument-LOQ	0.005	0.034	0.017
Sample weight (g)	0.1 g	0.5 g in 40 mL	
Method-LOD	0.01 µg/kg	0.80 µg/kg	
Method-LOQ	0.05 µg/kg	2.72 µg/kg	

*Based on volume of the sample loop = 0.5 mL

Table S3 The analysis results of T-Hg in marine sediment CRMs

Marine sediment CRM	DTD-AAS			Acid-CVAAS		
	%Recovery	%RSD	*n*	%Recovery	%RSD	*n*
MESS-3	97.3 ± 2.1	2.2	12	99.0 ± 6.7	6.8	22
PACS-2	94.8 ± 6.2	6.5	11	100.7 ± 8.5	8.4	16

Table S4 T-Hg concentrations (µg/kg dry weight, *n* = 2) for intact marine sediment samples from the 4 sediment cores collected in the Gulf of Thailand and analyzed using DTD-AAS method

Sectioned sample (cm)	Core 14		Core 22		Core 29		Core 35	
	Average	%RPD	Average	%RPD	Average	%RPD	Average	%RPD
0 – 1	32.95	4.1	28.23	0.4	27.98	2.9	20.64	2.3
3 – 4	32.45	0.3	27.80	3.6	27.91	3.5	20.19	6.2
6 – 7	31.41	5.4	25.58	8.1	26.75	0.5	19.94	1.1
9 – 10	29.82	5.5	25.37	6.4	25.66	2.5	19.41	0.9
12 – 13	28.62	8.3	23.44	2.7	27.25	13.1	19.08	5.4
15 – 16	25.94	5.4	23.08	0.0	24.48	0.8	18.24	3.5
18 – 19	27.29	13.5	21.36	0.1	24.40	1.0	17.95	1.2
21 – 22	24.67	13.8	20.96	0.9	21.85	4.8	17.72	0.5
25 – 26	24.16	8.3	20.25	3.7	19.36	5.2	17.58	1.0
30 – 31	24.33	13.6	19.54	0.5	21.10	9.5	17.08	0.2
35 – 36	23.74	0.9	19.57	4.6	18.22	2.7	16.26	0.6
40 – 41	–	–	19.24	0.7	18.68	4.1	16.19	3.6
45 – 46	–	–	19.26	0.8	19.30	9.4	16.50	3.4
50 – 51	–	–	20.09	1.8	19.04	7.8	16.46	0.2

Table S5 T-Hg concentrations (μg/kg dry weight, n = 3) for intact marine sediment samples from the 4 sediment cores collected in the Gulf of Thailand and analyzed using acid-CVAAS method

Sectioned sample (cm)	Core 14		Core 22		Core 29		Core 35	
	Average	%RSD	Average	%RSD	Average	%RSD	Average	%RSD
0 – 1	32.10	10.2	28.79	6.5	25.56	10.3	24.35	5.9
3 – 4	30.86	8.7	28.09	4.6	28.70	4.6	22.90	2.8
6 – 7	34.17	6.3	26.18	2.5	29.60	2.3	20.22	9.4
9 – 10	29.69	5.2	26.76	8.8	28.80	5.0	18.09	3.1
12 – 13	28.01	6.7	26.03	1.5	30.44	4.2	18.26	1.0
15 – 16	27.34	3.5	24.41	6.7	21.07	3.5	18.73	7.0
18 – 19	27.14	6.3	22.34	10.0	23.92	9.2	17.47	7.0
21 – 22	23.25	4.1	20.82	3.0	23.95	4.5	18.28	7.1
25 – 26	22.86	12.0	21.30	5.2	19.49	6.5	17.21	3.4
30 – 31	27.50	6.4	18.54	6.0	19.02	9.7	16.63	6.5
35 – 36	24.51	2.7	19.22	7.8	21.05	7.3	18.09	5.3
40 – 41	–	–	18.32	4.3	15.97	2.4	17.11	3.2
45 – 46	–	–	19.22	5.0	19.90	8.3	16.42	4.1
50 – 51	–	–	21.11	2.2	19.80	10.9	18.20	3.5

Table S6 Statistical analysis for the comparison between to the two analysis methods via Pearson correlation and paired t-test (α = 0.05)

	Acid-CVAAS	DTD-AAS
Mean	22.97738592	22.53532604
Variance	22.69064262	20.1297451
Observations	53	53
Pearson Correlation	0.940107347	
Regression Statistics (P-value)		1.71538×10^{-25}
Hypothesized Mean Difference	0	
df	52	
t Stat	1.981938202	
P(T<=t) two-tail	0.052783062	
t Critical two-tail	2.006646805	

Table S7 T-Hg concentrations in the sediment cores before and after 1961

Core #	T-Hg by DTD-AAS [μg/kg] carbonate-free basis			
	Before 1961		Since 1961	
	Average ± SD	Range	Average ± SD	Range
14	27.54 ± 1.52	25.95 – 30.12	34.33 ± 2.07	31.66 – 36.68
22	23.33 ± 2.40	20.90 – 28.33	30.43 ± 1.64	28.56 – 31.62
29	23.55 ± 1.44	21.61 – 25.05	31.34 ± 3.16	24.52 – 34.05
35	18.69 ± 0.42	18.26 – 19.31	21.41 ± 1.36	19.75 – 23.41
BPK	47.03 ± 1.10	44.49 – 48.45	49.51 ± 2.15	46.07 – 52.76

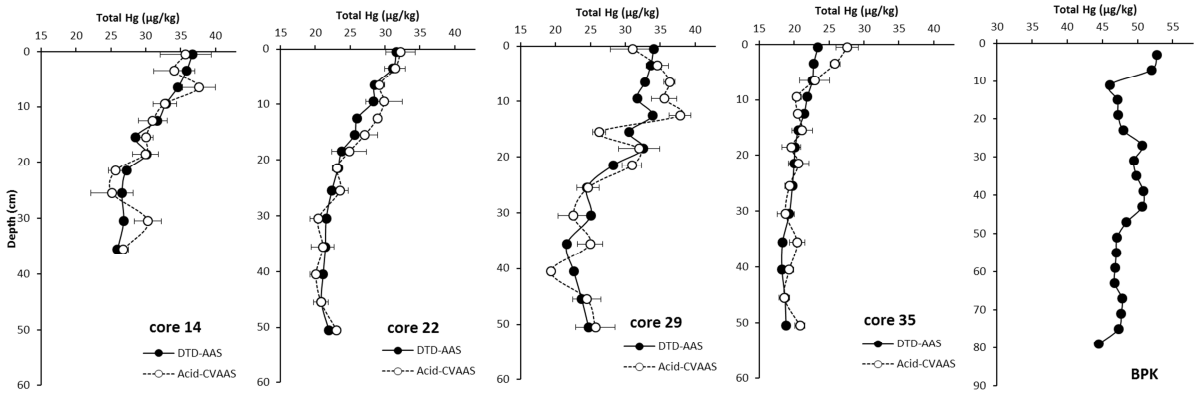

Fig. S1 Comparison of T-Hg concentration (μg/kg) in the carbonate-free sediment samples analyzed by using compared DTD-AAS method and acid-CVAAS method. Note that T-Hg contents in core BPK were analyzed by DTD-AAS only and axis scales for core BPK vary from the remaining four cores

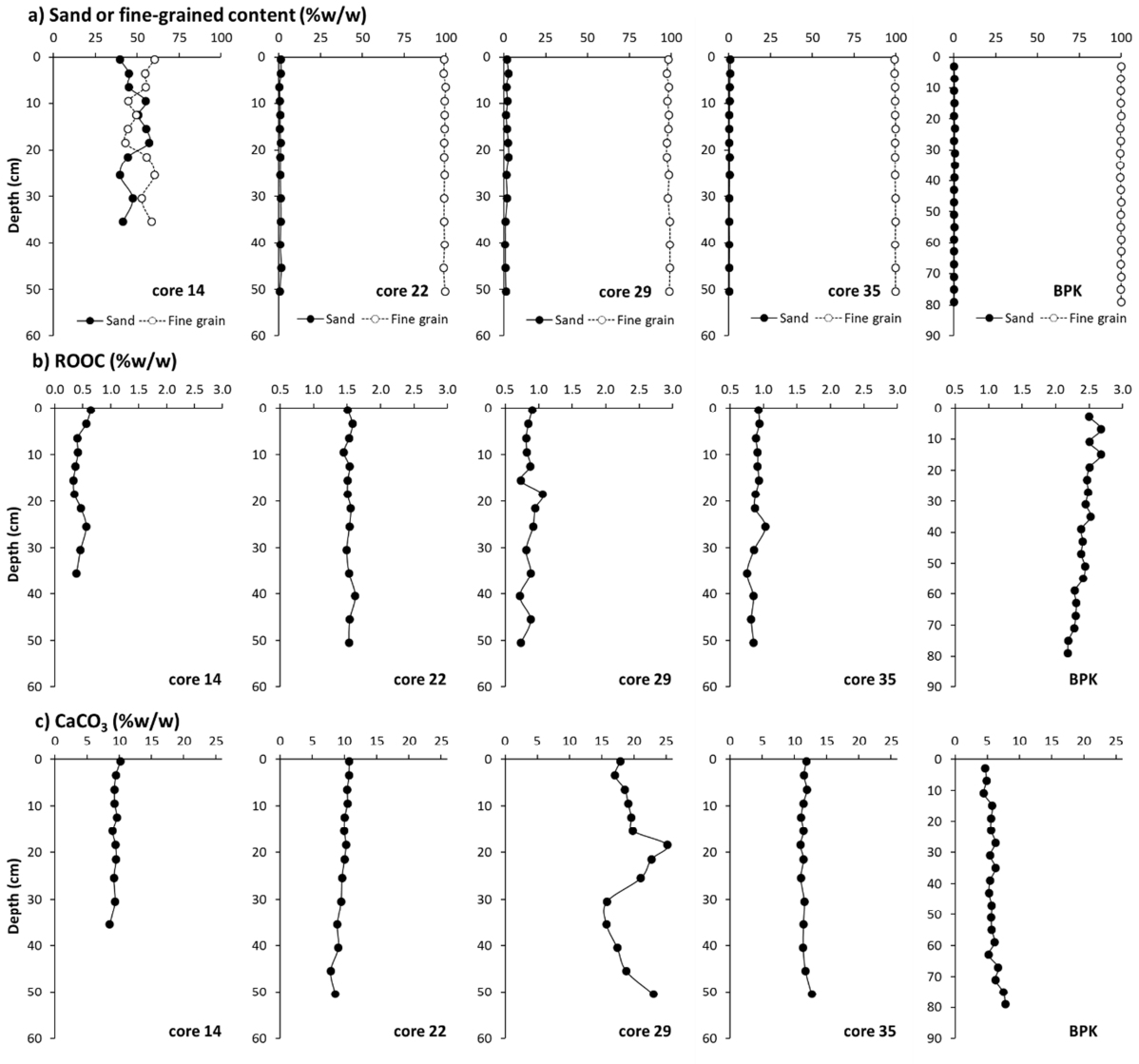

Fig. S2 Vertical profiles of a) grain sizes, b) ROOC, and c) $CaCO_3$ in the sediment cores

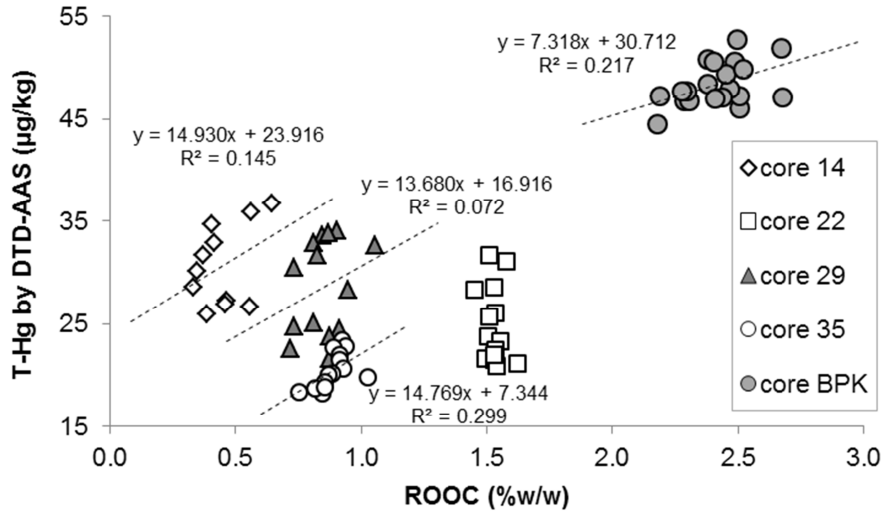

Fig. S3 Correlation between T-Hg (analyzed by the DTD-AAS method) and ROOC content